Pergamon

Cement and Concrete Research 33 (2003) 215–222

CEMENT AND CONCRETE RESEARCH

Three-dimensional microstructure analysis of numerically simulated cementitious materials

G. Ye*, K. van Breugel, A.L.A. Fraaij

Delft University of Technology, Faculty of Civil Engineering and Geosciences, P.O. Box 5048, 2600 GA Delft, The Netherlands

Received 7 February 2002; accepted 28 April 2002

Abstract

In order to predict the transport properties of porous media, such as permeability and electrical conductivity of cementitious materials, a better understanding of the microstructural characteristics, including the geometrical and topological properties, is required. In this contribution, the microstructure of cementitious materials is simulated by using the cement hydration model HYMOSTRUC. In this computer-based numerical model, the hydrating cement grains are modeled as gradually growing spheres, which become in contact while growing. The simulated porous medium can be described as a series of sections taken from three orthogonal directions, in which each unit (pixel) is filled either with a solid or a fluid phase (pores). Various algorithms based on a random walk process are utilized to determine the local geometrical information, such as gravity center's coordinate, perimeter and area of each individual pore. The percolating path of the fluid in three dimensions is traced by using an overlap algorithm. Both three-dimensional (3D) geometrical information and topological space characterization including branch node network and genus of the pores are derived. Calculation results of these algorithms are compared with results obtained by other microstructural models at various degree of hydration.

Keywords: Portland cement; Hydration products; Microstructure; Image analysis modeling

1. Introduction

In order to investigate the development of the microstructure of a cementitious material, such as the volume fraction and the percolation threshold of either the solid or the porous phase, and in particular, the transport properties, such as moisture flow and water permeability, a quantitative description of geometrical and topological properties of the porous structure is needed.

The experimental determination of the microstructure of porous cementitious materials is quite complicated. This is due to the wide range of pore sizes of cementitious materials and difficulties with the sample preparation. To this end, numerical simulation of the microstructure of cementitious materials has attracted increasing attention in the past decades. However, accurate simulation of the microstructure presupposes that we understand the kinetics of cement hydration and that we are able to describe the reaction process with an algorithm. On the other hand, it is also necessary to precisely describe these simulated microstructures.

A digital-image-based model was developed by Bentz and Garboczi [1]. The advantage of this model is that it allows the direct representation of multiphase and non-spherical cement particles. A percolation theory of pores/solid was utilized to analyze the connected fractions of different phases in three dimensions. More recently, based on the continuum representation approach, an integrated particle kinetic model for three-dimensional (3D) simulation of the evolution of tricalcium silicate microstructure during hydration was reported by Navi and Pignat [2]. Using a technique of morphological thinning and partitioning of the void space, the 3D microstructural properties, such as pore size distribution, volume-to-surface ratio and connected pore fraction, can be deduced.

However, as emphasized by Lymberopoulos and Payatakes [3], the transport properties, such as permeability, strongly depend on the sizes of narrow pores through which the fluid must flow. The predictions of permeability are usually parametric relationships that are required in the

* Corresponding author. Tel.: +31-15-27-81662; fax: +31-15-27-85895.

E-mail address: ye.guang@citg.tudelft.nl (G. Ye).

0008-8846/02/$ – see front matter © 2002 Elsevier Science Ltd. All rights reserved.
PII: S0008-8846(02)00889-X

quantitative description of the geometry and topology of the microstructure, especially in a network model. It is evident that geometrical parameters, such as percolation threshold of porosity and pore size distribution, are not sufficient for describing the transport behavior in porous media. In fact, the topological parameters, including the throat and the interconnectivity of pore space channels, play a dominant role in the permeability of a cementitious material.

In this paper, the 3D cement hydration model HYMOSTRUC [4] was used to simulate the microstructure of cement paste. A serial sectioning algorithm and an overlap criterion were employed for the determination of the pore structure. A newly developed visualization technique allows a better understanding of the development of microstructure, including the pore structure.

2. Simulation and visualization of microstructure of cementitious materials

The numerical model HYMOSTRUC [4] was developed for simulation of the reaction process and of the formation of the microstructure in hydrating Portland cement. In this model, the degree of hydration is simulated as a function of the particle size distribution and of the chemical composition of the cement, the water/cement (w/c) ratio and the reaction temperature.

In a computer-digitized format of HYMOSTRUC, the cement particles are modeled as digitized spheres randomly distributed in a 3D body and the hydrating cement grains are simulated as growing spheres [4,5]. As cement hydrates, the cement grains gradually dissolve and a porous shell of hydration products is formed around the grain. This results in an outward growth or "expansion" of the particles. The hydrates around the cement grains first cause the formation of small isolated clusters. Big clusters are formed when small cement particles become embedded in the outer shell of other particles, which promotes the outward growth of these particles (Fig. 1). As hydration progresses, the growing particles become more and more connected. The material changes from the state of a suspension to the state of a porous elastic solid.

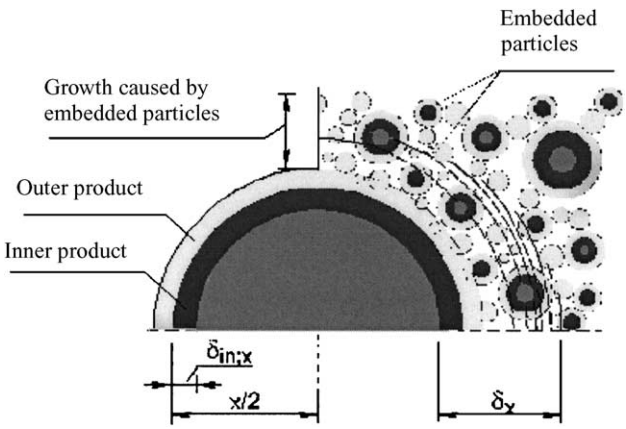

Fig. 1. Formation of a microstructure in hardening cement paste [4].

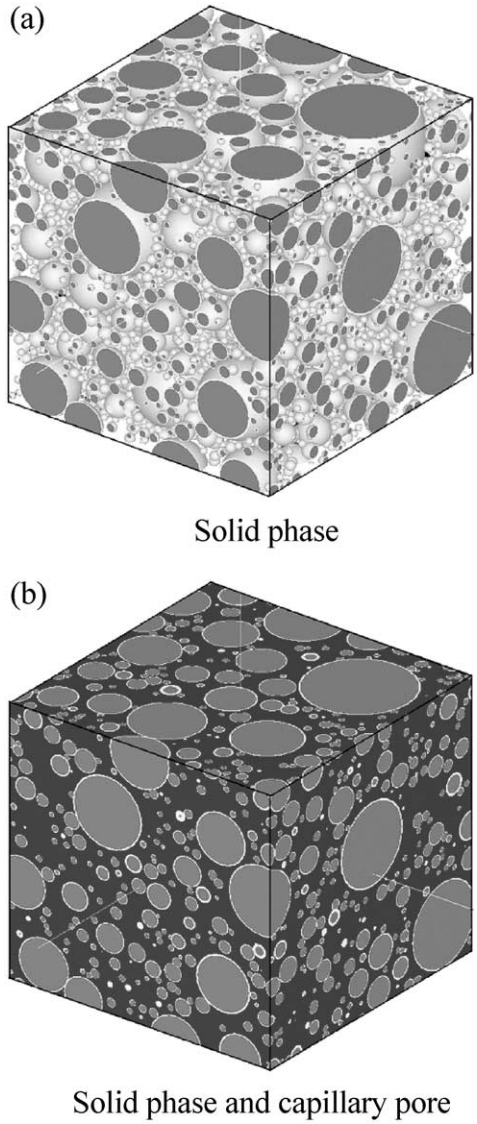

Fig. 2. Simulated cement paste with w/c ratio 0.4. After 11 h hydration, degree of hydration 16%. Sample size is $100 \times 100 \times 100$ μm^3.

As shown in Fig. 2a, a cube of hydrating paste was simulated with w/c ratio 0.4 and curing temperature 20 °C. For the adopted cement particle size distribution, 6194 particles were randomly distributed in a $100 \times 100 \times 100$ μm^3 cubic space. The minimum diameter of cement particles was 2 μm and the maximum diameter was 45 μm. Fig. 2 shows the hydration stage at 11 h, when the degree of hydration reaches 16%. The yellow color represent the outer products, the red color the inner products, gray color denotes unhydrated cement cores and the blue color is considered as capillary pores (Fig. 2b).

A CSG [6] algorithm was used for the visualization of the pore structure. In Fig. 3a and b, the simulated capillary

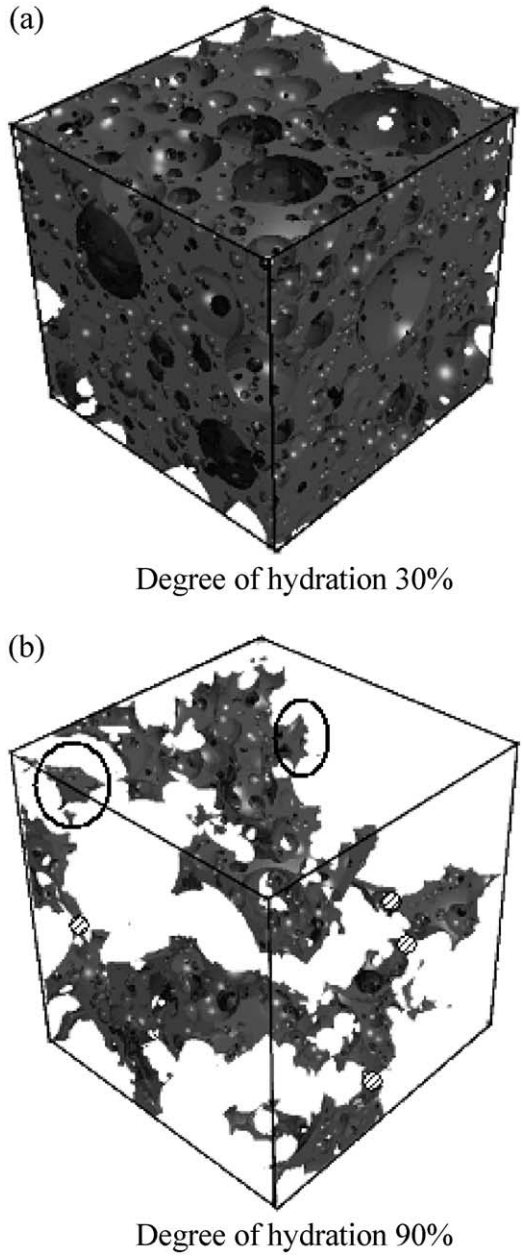

Fig. 3. Simulated capillary pore network with water/cement ratio 0.4.

porous network at degrees of hydration of 30% and 90%, respectively, are shown. A number of special features can be individuated in these visualized pore structures. Firstly, it is obvious that the capillary pores are very irregular; therefore, if the model represent the truth, it is not appropriate to consider these pores as cylindrical pores, as assumed for example in mercury intrusion porosimetry. Secondly, from the view of a network model, as observed from the region marked with ellipses in Fig. 3b, the isolated pores and dead-end pores will not contribute to the transport properties. Another important characteristic is indicated with white dots in Fig. 3b, this so-called necks or throats. These necks or throats are the critical links for water transport in the porous network.

3. Analysis of the simulated microstructure

Identification and specification of the size distributions for pore bodies and pore necks, and interconnectedness of pore network are the most difficult components in the porous materials, both for a real porous medium and for a simulated porous structure. As mentioned by Serra [7], no applications of the available techniques of mathematical morphology could be found to analyze a porous microstructure. Details of the topological concepts needed to identify pore bodies and pore necks are given by Dullien [8], where discussions of pore-structure parameters, including the definitions of topological concepts such as the genus and its dependence on other topological properties, were presented. Algorithms for determining these topological factors, from which pore body to pore neck networks are constructed, are described by Dullien [9], mostly in the context of the serial sectioning work of MacDonald et al. [10,11]. Alternatively, Lymberopoulos and Payatakes [3,12] proposed a procedure for estimating the genus from serial sections. The obvious advantage of their method is that only two closely spaced serial section data were used, which significantly reduces the amount of data that has to be stored, with little loss of information. Their method has been used as the basis for the present development.

3.1. Scanning the 3D microstructure by serial sectioning method

The serial sectioning method starts with scanning the simulated 3D microstructure from three orthogonal directions layer by layer. Fig. 4a and b shows the solid phase sections and pore phase sections, respectively.

In order to characterize the features of each 2D section, the procedure starts from checking neighboring pixels with the aid of an array that contains the coordinates of neighboring pixels relative to the pixel currently analyzed. The advantage is that the check can be done with a simple one-dimensional array. In the next layer, every pixel is checked once again to determine if a pixel is part of a pore and to number the pores accordingly. Whenever an edge is found, a new pore is created and given a new number. Further, a recursive function for calculating the perimeter is called. By tracing the edge and marking each edge pixel, the length of the perimeter is obtained. If the program finds another edge pixel that belongs to a pore that already has a number, it means that this pore is a part of the same pore and therefore the pore number is changed to that particular pore's number. The perimeter and the pore number are saved. Another recursive function for calculating the area is called, which will calculate not only the edge pixels, but also all pore (or solid) pixels to count their area. When the pore is not connected to any other pore, it is given a new pore number, higher than the last pore number that was recorded. The pore data is then connected to the general list of pores, to the appropriate branch according to its pore number and their layer where it was found. When a new

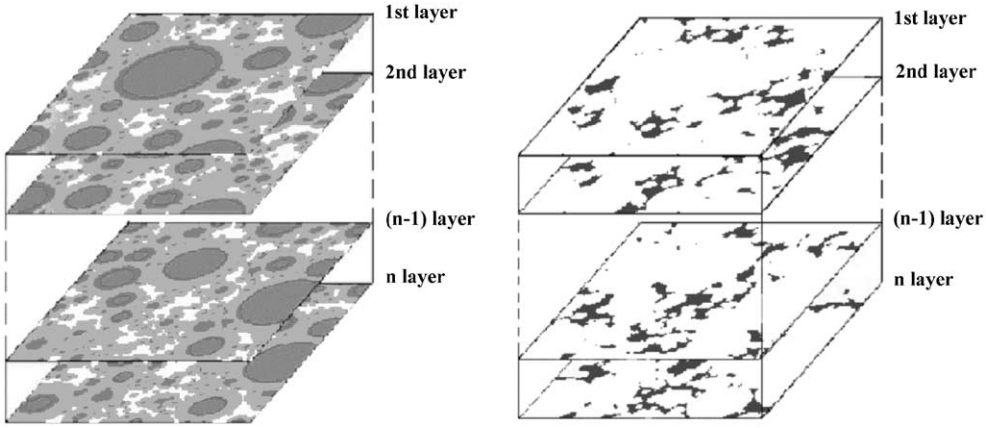

Fig. 4. The simulated microstructure can be considered as serial sections (left: solid phase, right: porous phase).

pore with the same pore number and the same layer is found, the object is discarded, but the area and perimeter information is added to the existing data.

The hydraulic radius is a useful measure of "size" in the case of irregularly shaped cross sections [13]. According to the definition given by Dullien [9], the hydraulic radius R_H can be computed as:

$$R_H = A/P \tag{1}$$

where A is the cross-sectional area of a pore and P is the length of its perimeter.

The coordination of the gravity center of each pore can be approximately computed by:

$$X = \text{sum}(x)/\text{count} \tag{2}$$

$$Y = \text{sum}(y)/\text{count} \tag{3}$$

where X and Y are the coordinates of the gravity center for a pore on a certain layer Z, sum(x) and sum(y) are the summation of the x coordinates and the y coordinates of each pixel belonging to one pore and the "count" is the number of pixels in this pore.

Thus, each individual pore with its 2D features, including perimeter, area and gravity center coordinates, is stored and ready for further determination of interconnectedness.

3.2. Determination of the interconnectedness of 2D features and genus

In order to determine whether two or more pore features on serial section are interconnected or not, the overlap criterion is applied. The overlap criterion was given by Ref. [3]. The overlap between two 2D features exists if the features belong to adjacent layers and at least one perpendicular line exists on which both features have the same color. The most important topological parameter is the genus number, since it is a measure of the alternative paths, which are available to fluid flow, diffusion, etc., in porous media. According to Ref. [3], the genus number is defined as the maximum number of non-interesting closed curves that can be made upon the surface of a structure without separating it into disconnected parts. It is equal to the number of distinct holes through a structure, or the maximum number of cuts that a multiply connected structure can undergo in order to form a simply connected one.

The overlap criterion and of the genus number largely depends on the resolution of pixels and layer depth. The higher the resolution, the higher the accuracy that can be obtained for an acceptable CPU calculation time and a reasonable representation of physical size of the sample. In this study, a cubic space of 100 μm^3 was represented by $400 \times 400 \times 400$ pixels. The resolution of the pixel is 0.25 μm and the layer thickness equal to the resolution of the pixel.

The determination of the interconnectedness between the features on the serial sections is achieved with the linked-list network structure shown in Fig. 5. An example of analyzed pore structure is shown in Fig. 6.

In this linked-list structure, each pore is a 3D-pore set and each pore in the branch consists of objects from 3D pore structure data. A cumulative function automatically puts the data in their right place according to pore ID number and their layer number to this linked-list structure. Next, the current pore ID is compared with the upper layer number; if the ID number is larger, the new data is a new pore and a new

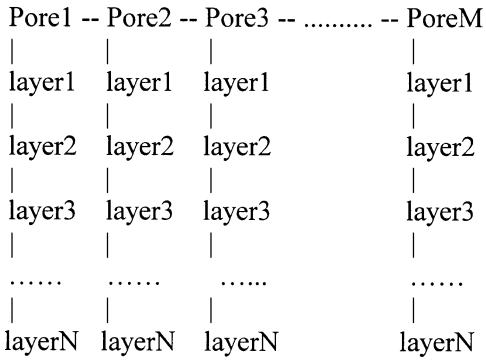

Fig. 5. Linked-list network structure for determination of the interconnectedness on serial section.

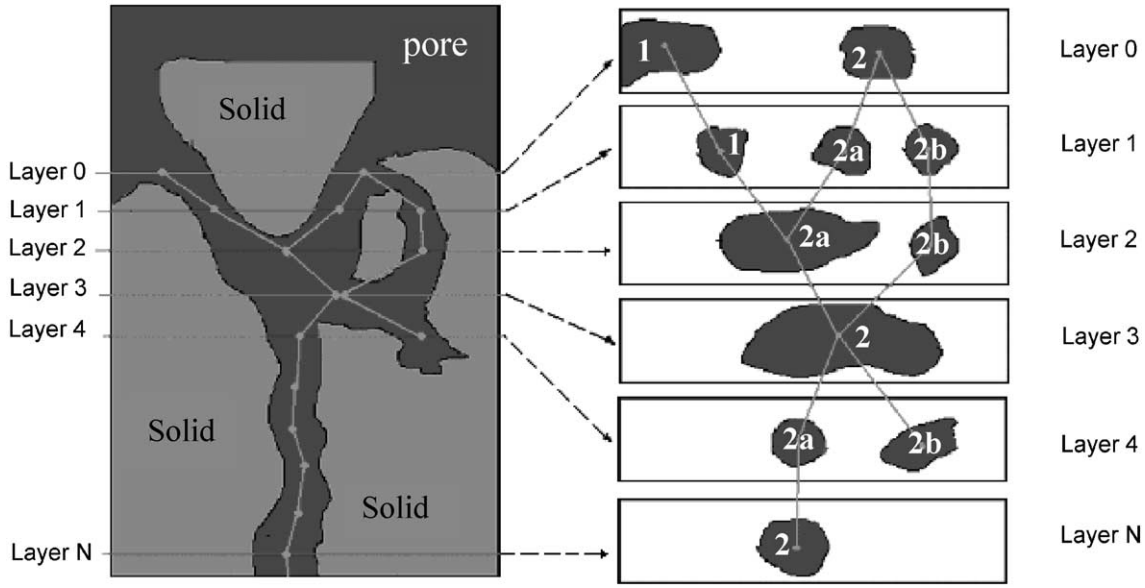

Fig. 6. Example of determination of the interconnectedness of 2D features.

pore is created and added to the end of the list. If this pore ID is smaller than the top layer ID, the program searches for the correct place to keep the number in order and then makes a new node and puts it between existing nodes.

A move pores function is used for multilayer analysis if two pore, that at first seem to be separated, are found to merge on subsequent layers. Then a new node is recorded and all the data need to be removed. Afterwards, all the nodes from one linked-list structure are transferred to the appropriate linked-list structure object and the empty branch is discarded.

In hydrating cementitious materials, the pore structure changes with progress of the hydration process. The calculation results show that more than 95% pores are interconnected in a sample with a w/c ratio 0.4, even at degree of hydration of 0.9. Therefore, the channels that are not throughout the whole sample will not be taken into account in the calculation of genus number. A modified formula by Lymberopoulos and Payatakes [3] for computing the topological parameter genus G was applied.

$$G_{\min} = c_{\text{in}} - f + N_{\text{in}}, \tag{4}$$

$$G_{\max} = (c_{\text{in}} + c_{\text{out}}) - (f + 1) + ((N_{\text{in}} - N_{\text{out}}) + 1), \tag{5}$$

where c_{in} is the number of connections between overlapping features of pores or solid, c_{out} is the number of pore channels intersected by the sample boundaries, f is the number of pores, N_{in} is the overall number of separate networks and N_{out} is the number of separate networks, which have access to the boundaries of the sample.

For example, as shown in Fig. 6, we already have Pores 1 and 2 in Layer 0. During the analysis of Layer 1, three pores are found. One of them is found to overlap with Pore 1 and the other two are overlapped with Pore 2. However, since these three pores are not connected to each other in this layer, the Pore ID 1 and 2 are assigned. Subsequently, we find that Pore 1 is connected with Pore 2 in Layer 2; a node is found and the data of Pore 1 detached from the main list. A new ID (2) is assigned and then added again to the list, as a part of the Pore 2 branch. After the analysis outlined above, the number of connections between overlapping features c_{in} is 15, the number of pore channels intersected by the sample boundaries c_{out} is 3, the number of pores f is 15, the overall number of separate networks N_{in} is 1 and N_{out} is 1. According to Eqs. (4) and (5), the calculated genus number $G_{\min}$ is 1 and $G_{\max}$ is 3.

The liquid flow channel can be obtained by tracing a line through the coordination of the gravity center of each pore.

4. Results and discussion

Two numerical simulation of cement paste have been performed. Table 1 shows the input parameters for the

Table 1
Input parameter for the numerical experiments

Sample no.	w/c ratio [−]	Sample size (μm)	Particle size (μm)	Particle no.	Image size (pixel)	Pixel resolution (μm/pixel)	Number of layers
1	0.3	100	2–45	7123	400	0.25	400
2	0.4	100	2–45	6149	400	0.25	400

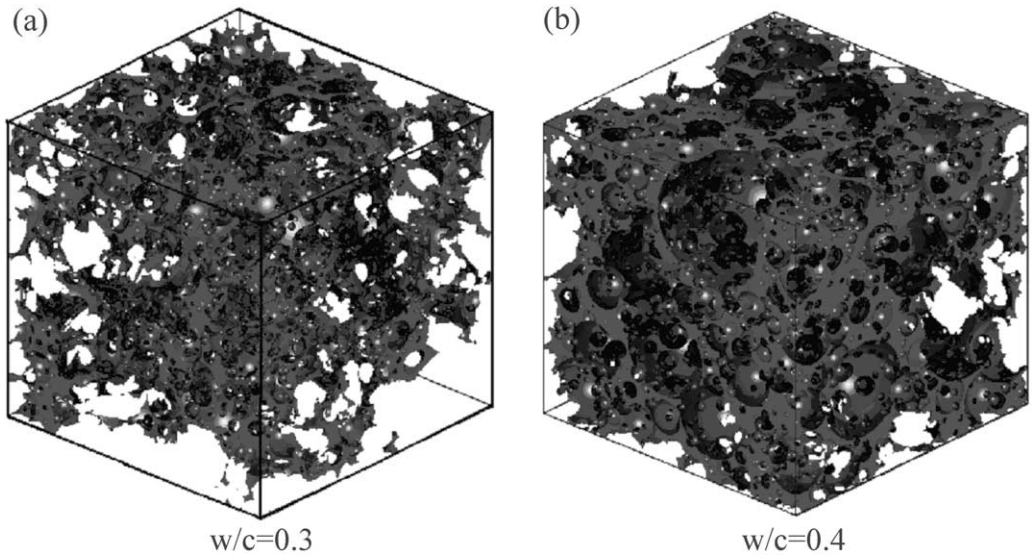

Fig. 7. Capillary pore structure in paste with different w/c (α=.70).

simulation. Curing temperature is 20 °C. The main variable is the w/c ratio, i.e., 0.3 and 0.4.

The simulated pore structures are illustrated in Fig. 7a for a w/c ratio 0.3 and Fig. 6b for a w/c ratio 0.4, both at a degree of hydration 0.7. It is obvious that at the same degree of hydration, the sample with the lower w/c ratio shows less porosity than the sample with a higher w/c ratio. The calculated result revealed a capillary porosity of 2% for w/c 0.3 and 11% for w/c 0.4.

4.1. Development of microstructure: percolation threshold of the solid and the capillary pore phase

Fig. 8 shows results for the percolation threshold of the solid and capillary porosity for two different w/c ratios. The solid percolation threshold was found at a degree of hydration 0.02 in the case of w/c ratio 0.3 and at degree of hydration 0.025 in the case of w/c ratio 0.4. Afterwards, the connected solid phase shows a quick increase and all solid particles are connected with each other at a degree of hydration of 0.25. These phenomena have been found to be in fairly good agreement with an experimental ultrasonic pulse velocity (UPV) test performed on a cement paste with the same w/c ratio [14]. In the experiments, a sudden change of UPV was reported after 3 h hydration. After 30 h, the UPV increased only slowly until the end of experiment. Similar phenomena also can be found in Refs. [15–17].

For the evolution of the capillary porosity, Fig. 8 shows that almost all capillary pores are connected with each other up to a degree of hydration of 0.70. A value of 3.5% of the capillary porosity percolation threshold is found in both samples, corresponding to a degree of hydration 0.91 for the sample with w/c ratio 0.4 and a degree of hydration 0.63 for the sample with w/c ratio 0.3. The evidence of a constant value of capillary porosity percolation threshold is in good agreement with simulations with the NIST model [18].

Fig. 9 shows a comparison, at the same w/c ratio 0.4, of the fraction of solid/capillary porosity between the NIST

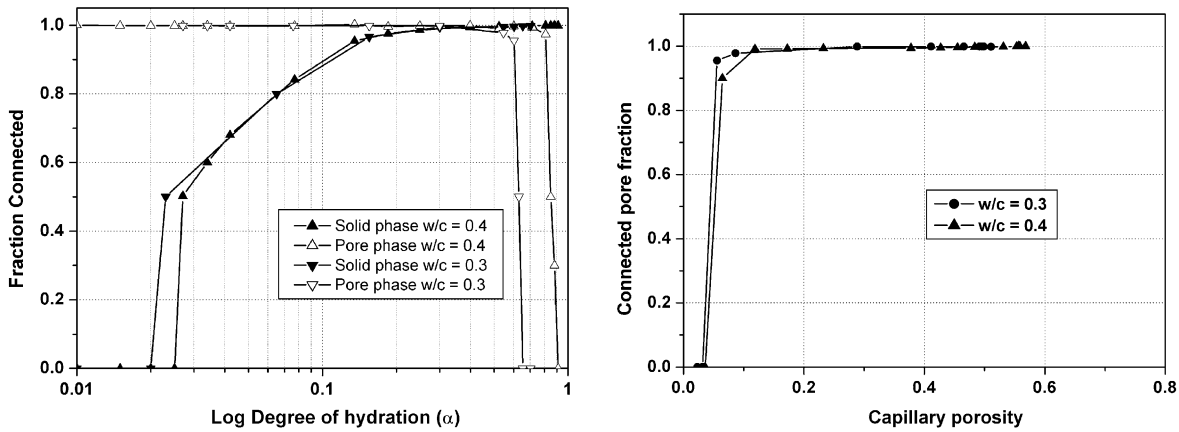

Fig. 8. Development of microstructure in cement paste with two different w/c ratios (left: phases connected fraction as function of degree of hydration, right: connected pore fraction as function of capillary porosity).

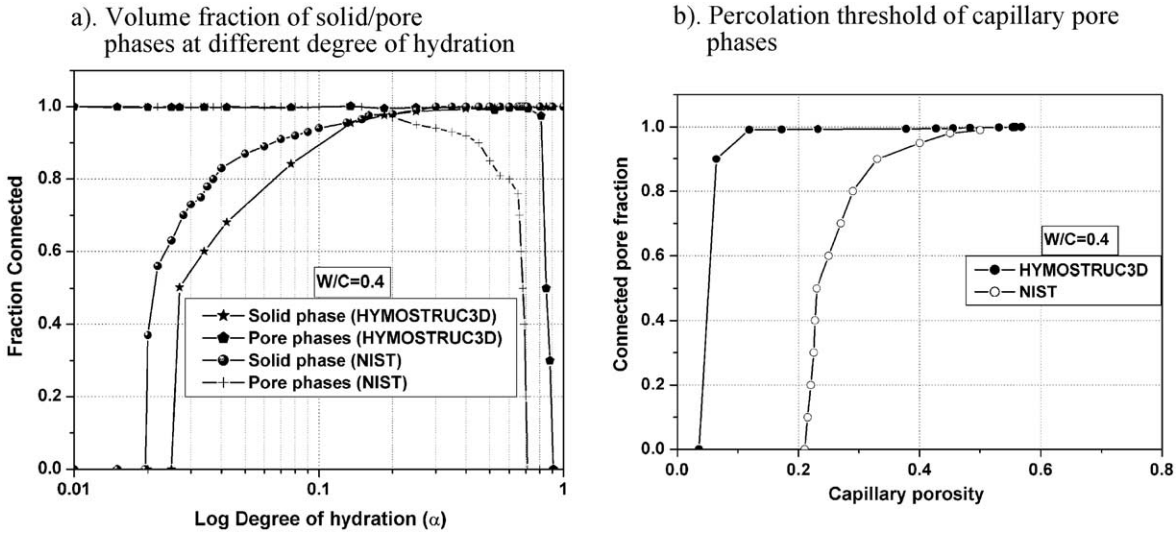

Fig. 9. Comparison between different simulation models.

model and the HYMOSTRUC3D model. Note that in the NIST model, only four sizes of particles with diameter of 3, 9, 13 and 19 pixels were used, the physical size of sample was $100 \times 100 \times 100$ μm^3 and the resolution in this case was 1 μm/pixel [18]. In the HYMOSTRUC3D, a continuous particle size distribution, between minimum size 2 μm and maximum size 45 μm was used, the physical size of sample was the same as the NIST simulation, while the resolution was 0.25 μm/pixel.

A similar development of solid phases can be found in both models. As discussed previously, these two models both reach a solid phase percolation threshold at a degree of hydration around 0.02–0.03. At a degree of hydration of 0.20–0.25, nearly all solid phases are connected. However, significant differences on the evolution of the capillary pore structure between the two models are shown in Fig. 8b. Firstly, the capillary porosity percolation threshold is found to be about 20–22% in the NIST model [18], whereas in the HYMOSTRUC3D, the percolation threshold of the capillary porosity is found at about 3.5%. Secondly, the porosity percolation threshold occurs in the NIST simulation at a degree of hydration of 0.70, but in HYMOSTRUC3D, the capillary porosity percolation threshold occurs much later, at a degree of hydration around 0.90 (Fig. 9a).

Why are the differences in capillary porosity so pronounced in the two models? To answer this question, we must understand the principle of both hydration models. In the NIST model, the different cement components are simulated as different sets of digital pixels; when C_3S hydrates, a cellular automaton model is applied, in which the reactants (pixels) dissolve from their matrix and walk around the capillary water space. When two reactants meet at a certain place, a chemical reaction occurs and the reaction products will be located in this place. In consequence, a lot of smaller capillary pores are blocked by these "walking around" hydration products. Another important factor that affects the capillary porosity percolation is the digital resolution. A complete discussions on the influence of image resolution in the NIST model is presented in Ref. [18]; it is shown that the higher the resolution, the lower the capillary percolation threshold. When the resolution changes from 1 to 0.25 μm/pixel, the capillary percolation threshold decreases from 22% to 11% porosity. The latter value is close to the 3.5% porosity found with HYMOSTRUC3D.

4.2. Connectivity of capillary pore structure

Calculations of the interconnectedness were performed for sample with the w/c ratio of 0.3 and 0.4, at a degree of hydration of 0.50. Table 2 includes the most important calculation results. The evolution of the calculated value of the genus/volume versus the sections examined is shown in Fig. 10. The upper and lower limits of the genus for the sample with w/c = 0.3 are $G_{min} = 361$ and $G_{max} = 448$. For the sample with w/c = 0.4 are $G_{min} = 753$ and $G_{max} = 904$, respectively.

It is clear that at the same degree of hydration, the genus number for the sample with w/c = 0.3 is larger than that of

Table 2
Calculation of the connectivity of capillary pore structure

w/c	Degree of hydration [−]	Total porosity (%)	Connected porosity (%)	Connected porosity fraction (%)	Average pores number in 2D	Average links between two layers	G_{min}	G_{max}
0.3	0.5	8.63	8.44	97.8	42.08	40.16	753	904
0.4	0.5	20.45	20.41	99.8	28.45	26.76	361	448

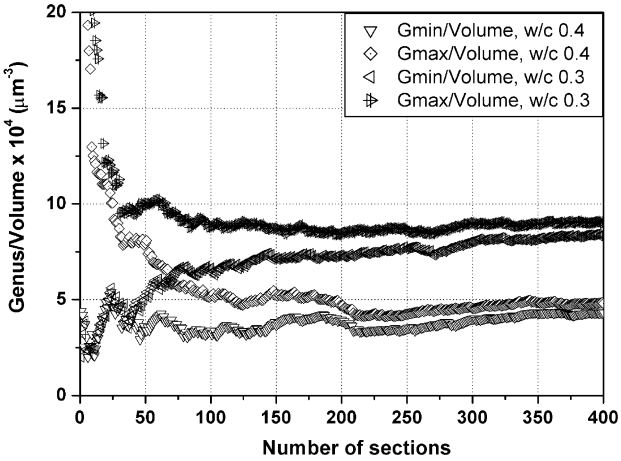

Fig. 10. Distribution of the calculated genus/volume versus the number of the sections examined. Sample with w/c = 0.3 and w/c = 0.4.

the sample with w/c = 0.4; a more complex fluid channel is formed in the sample with lower w/c. This is to be expected, since more pores are connected with each other in the sample with higher w/c ratio.

5. Conclusions

Based on the HYMOSTRUC cement hydration model, 3D microstructures of cement paste were simulated and visualized. A serial section algorithm with an overlapping criterion was used to characterize the 3D microstructure. This type of approach led to detailed information about various aspects of the capillary pore system (interconnectedness, branch to node network). From the pore structure analysis, however, it is shown that not only the geometrical but also the topological parameters will affect water permeability. The calculation of the genus number showed that the samples with lower w/c ratio have a more complex pore structure. According to the analysis of percolation threshold of phases, it has been shown that different cement hydration models reveal differences in the microstructure and particularly in the pore structure. Trends, however, are similar. The present study has shown that the percolation threshold of capillary porosity has a constant value in samples with different w/c ratio.

Further studies include the partition of the pore space by morphological skeletonization and application of this microstructural approach to study transport behavior. In particular, it will be studied how these microstructure parameters correlate with water permeability.

Acknowledgements

The authors wish to thank Mr. F.J.P. Chilperoort for his advice in programming and Mr. P. Lura for the useful discussion. The research was financially supported by the Dutch Technology Foundation (STW), which is gratefully acknowledged.

References

[1] D.P. Bentz, E.J. Garboczi, Digital-image-Based computer modeling of cement-based materials, in: J.D. Frost, J.R. Wright (Eds.), Digital Image Processing: Techniques and Application in Civil Engineering, ASCE, New York, 1993, pp. 63–74.
[2] P. Navi, C. Pignat, Three-dimensional characterization of the pore structure of a simulated cement paste, Cem. Concr. Res. 29 (4) (1999) 507–514.
[3] D.P. Lymberopoulos, A.C. Payatakes, Derivation of topological, geometrical, and correlation properties of porous media from pore-chart analysis of serial section data, J. Colloid Interface Sci. 150 (1) (1992) 61–80.
[4] K. van Breugel, Simulation of hydration and formation of structure in hardening cement-based materials, PhD thesis, Delft University of Technology, 1991.
[5] E.A.B. Koenders, Simulation of volume changes in hardening cement-based materials, PhD thesis. Delft University of Technology, 1997.
[6] M. Laszlo, Computational Geometry and Computer Graphics in C++, Prentice Hall, London, 1995.
[7] J. Serra, Image Analysis and Mathematical Morphology, Academic Press, London, 1982.
[8] F.A.L. Dullien, Porous Media: Fluid Transport and Pore Structure, 2nd ed., Academic Press, San Diego, 1992.
[9] F.A.L. Dullien, Characterization of porous media-pore level, Transp. Porous Media 6 (1991) 581–660.
[10] I.F. MacDonald, P. Kaufman, F.A.L. Dullien, Quantitative image analysis of finite porous media: I. Development of genus and pore map software, J. Microsc. 144 (1986) 277–296.
[11] I.F. MacDonald, P. Kaufman, F.A.L. Dullien, Quantitative image analysis of finite porous media: ii. Specific genus of cubic lattice models and Berea sandstone, J. Microsc. 144 (1986) 297–316.
[12] C.D. Tsakiroglou, A.C. Payatakes, Characterization of the pore structure of reservoir rocks with the aid of serial sectioning analysis, mercury porosimetry and network simulation, Adv. Water Resour. 23 (2000) 773–789.
[13] Z. Liang, M.A. Ioannidis, I. Chatzis, 3D pore structure based on skeletonization, Chem. Eng. Sci. 55 (2000) 5247–5262.
[14] G. Ye, K. van Breugel, A.L.A. Fraaij, Experimental study of ultrasonic pulse velocity evaluation of the microstructure of cementitious material at early age, HERON 3 (2001) 161–168.
[15] B. Boumiz, C. Vernet, F.T. Cohen, Mechanical properties of cement pastes and mortars, Adv. Cem. Based Mater. 3 (1996) 94–106.
[16] H.W. Reinhardt, C.U. Grosse, Setting and hardening of concrete continuously monitored by elastic waves, The online Journal of Nondestructive Testing and Ultrasonics, http://www.ndt.net/article/grosse1/grosse1.htm, 1, No. 07 (1996).
[17] J. Rapoport, J.S. Popovics, K.V. Subramaniam, S.P. Shah, The use of ultrasound to monitor the stiffening process of Portland cement concrete with admixtures, ACI Mater. J. 6 (1997) 675–683.
[18] E.J. Garboczi, D.P. Bentz, The effect of statistical fluctuation, finite size error, and digital resolution on the phase percolation and transport properties of the NIST cement hydration model, Cem. Concr. Res. 31 (2001) 1501–1514.